



ChemComm

**Quantum Tunnelling Dominates Chloride Leaching from
Polyvinyl Chloride**

| | |
|---------------|--------------------------|
| Journal: | <i>ChemComm</i> |
| Manuscript ID | CC-COM-07-2024-003489.R2 |
| Article Type: | Communication |
| | |

SCHOLARONE™
Manuscripts

Quantum Tunnelling Dominates Chloride Leaching from Polyvinyl Chloride

Gbolagade Olajide and Tibor Szilvási*

Received 00th January 20xx,
Accepted 00th January 20xx

DOI: 10.1039/x0xx00000x

Chloride leaching/removal is a fundamental reaction of polyvinyl chloride (PVC), pertinent to PVC recycling and environmental impacts. We show that quantum tunnelling (QT) drives >90 % of chloride leaching from PVC to water at all environmentally relevant temperatures offering new insights into plastic degradation and transformation processes.

Polyvinyl chloride (PVC) is the world's third-most produced plastic, accounting for over 10 % of total plastics production,¹ and is used in wide-ranging applications including pipes, roofs, flooring, cables, valves, and medical equipment among others.^{2, 3} PVC pipes have even surpassed metal pipes as the dominant material for new water systems in the U.S.⁴ As PVC is in contact with water in most applications, concerns have been raised over the possibility of PVC leaching chemicals into water, such as chloride.⁵ In addition, plastic waste recycling efforts have also emphasized the necessity of chlorine removal for successful PVC upcycling.^{1, 3, 6} Previous studies have established that chloride leaching/removal proceeds via an E2 mechanism (Figure 1) in a basic environment.^{7, 8} The E2 mechanism involves a concerted abstraction of a proton by the hydroxide from a CH₂ group and a chloride ion leaving from the adjacent CHCl group. The reaction results in the formation of a C=C double bond in the polymer backbone, a water molecule, and a chloride ion. This E2 mechanism occurs when PVC pipes are in contact with alkaline soils or when PVC waste is recycled using NaOH.⁹

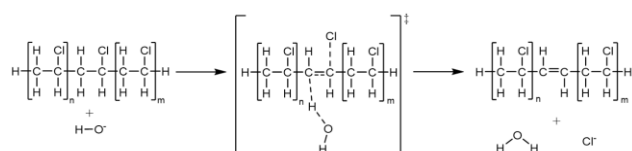


Figure 1. E2 mechanism of base-assisted chloride leaching from PVC

In this computational study, we consider the base-assisted chloride leaching from PVC to water with a focus on understanding the effect

of quantum tunnelling on the reaction. Quantum tunnelling (QT) is the phenomenon by which particles bypasses a potential energy barrier instead of surmounting it. QT provides an alternative pathway for reactants to transform into products and results in a higher reaction rate than that expected from thermal barriers.¹⁰ QT has been proven to be relevant for various reactions,¹¹⁻¹⁵ including enzyme catalysis,¹⁶⁻¹⁸ organic reactions,^{12, 19-23} and surface reactions²⁴⁻²⁶. QT has also been studied in a few free-radical mediated reactions of plastics such as free-radical polymerization^{27, 28} and poly- α -methylstyrene degradation,²⁹ using approximate methods such as the non-uniformized Wentzel-Kramers-Brillouin (WKB) approximation³⁰⁻³² and the one-dimensional Eckart tunnelling method³³. In this paper, we show using reliable canonical variational theory^{10, 34, 35} (CVT) calculations coupled with the small curvature tunnelling^{34, 36} (SCT) approximation that the base-assisted chloride leaching from PVC is dominated by QT at all practically relevant temperatures. By establishing the role of QT in chloride leaching from PVC, we show a practical example for tunnelling in plastic polymers in a non-radical mediated reaction and reveal that QT can contribute to plastic waste recycling.

We study the chloride leaching to water in a two-monomer unit computational model based on our benchmarking studies (see details in Section 1 of the Supporting Information). In our model, a hydroxide ion formally reacts with 1,3-dichlorobutane to form 1-chloro-2-butene, water, and a chloride ion. The transition state related to chloride leaching via the E2 mechanism is shown in Figure 2 at ω B97X-D(SMD=Water)/6-311+G(d,p)³⁷⁻⁴⁰ level of theory. The C-H bond at the transition state elongates from the equilibrium 1.095 Å to 1.359 Å, while the C-Cl bond distance changes from 1.841 Å to 2.157 Å. This suggests that the C-H and the C-Cl bond breaking are fully concerted, and Cl also actively participates in the transition state. The analysis of the imaginary mode indicates that the reacting hydrogen is displaced much more than the heavier chlorine as the displacement values in normal coordinates are 0.99 and 0.014 for hydrogen and chlorine, respectively. Notably, all other nuclei also undergo negligible displacement (< 0.1) relative to hydrogen. The displacement analysis suggests that the motion of the leaving hydrogen is critical during the chloride leaching process, hence, if QT is present in the reaction, it will be primarily driven by the involvement of the hydrogen in the elementary step.

Department of Chemical and Biological Engineering, The University of Alabama, Tuscaloosa, AL, 35487

Supplementary Information available: electronic structure and tunnelling calculations, geometries of optimized structures, and further details on the benchmarking of the basis set, functional, computational model, and tunnelling calculations. See DOI: 10.1039/x0xx00000x

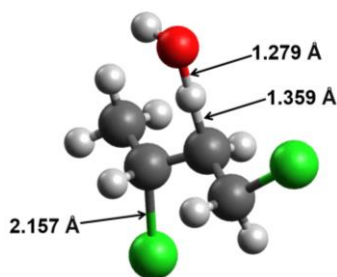


Figure 2. Transition state of the base-assisted chloride leaching in the two monomer-unit model at ω B97X-D(SMD=Water)/6-311+G(d,p) level of theory. Colour code: C – gray, H – white, O – red, and Cl – green.

We present the calculated standard-state energetics such as the reaction energy (ΔE_R), reaction Gibbs free energy (ΔG_R), electronic energy barrier (ΔE^\ddagger), and Gibbs free energy barrier (ΔG^\ddagger) in Table 1. ΔE_R (-20.6 kcal/mol) and ΔG_R (-30.9 kcal/mol) show that chloride leaching is thermodynamically favorable. The reaction has a relatively high barrier as indicated by ΔE^\ddagger and ΔG^\ddagger of 17.9 and 23.0 kcal/mol, respectively. ΔG^\ddagger suggests a low thermal reaction rate at room temperature; however, it is important to note that PVC pipes can be in contact with water for decades. We also find that some of the reaction energetics hint at a possible role of QT in the reaction. The large thermodynamic driving force together with the large imaginary mode of the transition state (1491 cm^{-1}) indicate a narrow barrier that is pertinent for QT as QT has an inverse dependence on barrier width.¹³

We explore the possible role of QT by carrying out CVT calculations coupled with the SCT approximation. We use well-converged parameters and compute the minimum energy path (MEP) long enough to completely cover the region where tunnelling occurs (see details in Section 1 of the Supporting Information). We calculate the semiclassical standard-state rate constant (k_{CVT}) as 2.8 s^{-1} and the QT-corrected rate constant (k_{SCT}) as 39.2 s^{-1} . Thus, the transmission coefficient (κ) is 13.9 at room temperature. Since QT rates depend on temperature, we calculate k_{CVT} , k_{SCT} , and κ from 70 K to 350 K for completeness (presented in Table S5 in the Supporting Information). Figure S1 shows k_{CVT} and k_{SCT} plotted against temperatures from 220 K to 350 K. We see that κ decreases with increasing temperature as expected (see Table S5 for more details) due to the stronger increase of thermal rates than tunnelling rates. Notably, κ is still 6.98 even at 350 K; thus, QT is important even at elevated temperatures. In Figure S2, we present an Arrhenius plot for k_{CVT} and k_{SCT} between 70 K and 350 K. $\ln(k_{\text{CVT}})$ shows a linear change throughout the temperature range. From about 220 K to 350 K, QT occurs from vibrationally-excited levels, so $\ln(k_{\text{SCT}})$ also changes linearly. However, below 200 K, QT mainly occurs from the vibrational ground state, reducing the temperature-dependence of k_{SCT} . Figure S3 magnifies the linear region of Figure S2, showing that the effective barrier determined from the Arrhenius plot of k_{SCT} is 13.3 kcal/mol, 3.2 kcal/mol lower than that obtained from the Arrhenius plot of k_{CVT} .

Table 1. Computed standard-state reaction energy (ΔE_R), reaction Gibbs free energy (ΔG_R), electronic energy barrier (ΔE^\ddagger), and Gibbs free energy barrier (ΔG^\ddagger) in kcal/mol; semiclassical rate constant

(k_{CVT}) and QT-corrected rate constant (k_{SCT}) in s^{-1} , the transition state imaginary frequency (ν_i) in cm^{-1} , SCT transmission coefficient (κ), and Tunnelling contributions (%Tun) for chloride leaching from the two monomer-unit model at ω B97X-D(SMD=Water)/6-311+G(d,p) level.

| | |
|---------------------|-----------------------|
| ΔE_R | -20.6 kcal/mol |
| ΔG_R | -30.9 kcal/mol |
| ΔE^\ddagger | 17.9 kcal/mol |
| ΔG^\ddagger | 23.0 kcal/mol |
| ν_i | 1491 cm^{-1} |
| k_{CVT} | 2.8 s^{-1} |
| k_{SCT} | 39.2 s^{-1} |
| κ | 13.9 |
| %Tun | 93 % |

We present the calculated vibrationally adiabatic ground-state energy curve of the minimum energy path (V_a^G) in Figure 3 to elucidate the contribution of tunnelling to the thermal reaction. The V_a^G curve is shown from $s = -4$ to $s = +4$ Bohr. $\text{amu}^{1/2}$, whereby s represents the mass-weighted reaction coordinate, and the colouring scheme refers to the tunnelling probability. We note that we observe some small (mostly below 50 cm^{-1}) imaginary frequencies along the V_a^G curve generally far away from the transition state and thus they should not affect the accuracy of our results. Furthermore, the plotted V_a^G curve approaches but does not reach the reactants and products; this is however unimportant as the shown V_a^G curve includes the region with non-negligible tunnelling probability (see Section 1 of the Supporting Information for more details). 96 % of all the tunnelling occurs in the shaded region magnified in the inset that spans from $s = -1.0$ to $s = +0.8$ Bohr. $\text{amu}^{1/2}$. Thus, all the tunnelling in the reaction occurs within 4.0 kcal/mol of the transition state and the tunnelling probabilities increase with decreasing barrier width,^{14, 41} reaching a maximum of 0.5⁴².

We analyse the tunnelling contribution (%Tun) to chloride leaching at various temperatures. Figure 4 presents the variation of %Tun between 220 K and 350 K and demonstrates that QT dominates chloride leaching reaction rates at all shown temperatures. At room temperature, QT is responsible for 93% of the chloride leaching rate and the thermal pathway only accounts for 7% of the reaction rate. %Tun decreases with increasing temperature similar to κ , however, it still accounts for 86% of the reaction rate at 350 K whereas it is responsible for 99+% of the reaction rate below 220 K (Table S5). Overall, Figure 4 indicates that QT provides the pathway for Cl^- to leach from PVC to water at all environmentally relevant temperatures.

To discern which atom is tunnelling, we perform kinetic isotope effects (KIE) analyses. On substituting deuterium for the leaving H, we calculate a H/D KIE of 23.18 at 298 K. At room temperature, a H/D KIE > 7 generally cannot be explained only by differences in the zero-point energy of the H and D isotopologues.¹⁴ We also calculate a $\text{Cl}^{35}/\text{Cl}^{37}$ KIE of 2.51 at 298 K on substituting the leaving Cl, and a $\text{C}^{12}/\text{C}^{14}$ KIE of 2.47 at 298 K on substituting the C bonded to the

leaving H. Our KIE analysis indicates that although QT in the reaction is driven by H-tunnelling, the other atoms might also contribute.

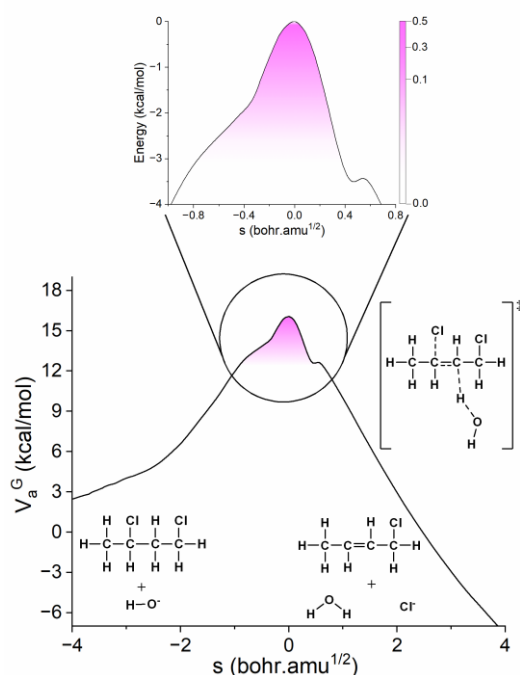


Figure 3. Vibrationally adiabatic ground-state energy curve of the minimum energy path (V_a^G) as a function of the calculated mass-scaled reaction coordinate (s) at ω B97X-D(SMD=Water)/6-311+G(d,p) level of theory for the two monomer-unit model. The vertical axis of the inset is the vibrationally adiabatic ground-state energy relative to the transition state, and the vertical axis of the figure is the vibrationally adiabatic ground-state energy relative to the reactant's potential energy. The values on the colour scale are the tunnelling probabilities.

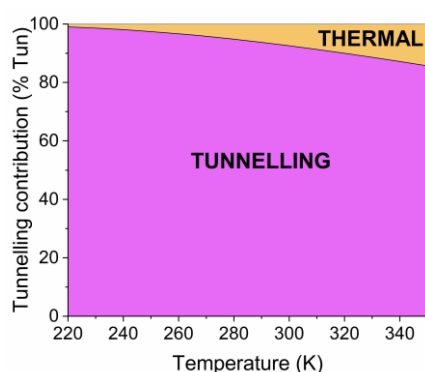


Figure 4. Tunnelling contribution (%Tun) to the reaction rate for the two monomer-unit model as a function of temperature in K.

To test the validity of the SMD model for OH⁻, we also carry out electronic structure and tunnelling calculations at the ω B97X-D(SMD=Water)/6-311+G(d,p) level on a two monomer-unit model with an explicit water molecule present (Section S4 of the Supporting Information). We show that an explicit water molecule does not affect our conclusions as %Tun changes only slightly to 86% at 298 K.

In conclusion, we provide computational evidence that QT plays a critical role in chloride leaching from PVC to water. We show that QT increases the reaction rate of chloride leaching by an order of magnitude by lowering the effective barrier by 3.2 kcal/mol. The present work highlights that QT is of a practical importance given the environmental relevance of chloride leaching. Our study also indicates that QT is an important phenomenon in PVC recycling, where removal of chlorine is desired under a controlled environment via the same reaction mechanism. We anticipate that QT may play a role in other plastic transformations relevant to the environmental impact of plastics and related global plastic recycling efforts, which are being explored further by our research group.

Conflicts of interest

There are no conflicts to declare

Data availability

Sample input files for electronic structure and tunnelling calculations, geometries of optimized structures, and further details on the benchmarking of the basis set, functional, computational model, and tunnelling calculations can be found in the Supporting Information.

Acknowledgement

G.O. and T.S. would like to acknowledge financial support from the National Science Foundation (NSF) under grants EFMA-2132133, EFMA-2029387, and 2339481. G.O. would like to acknowledge the financial support of the University of Alabama Graduate School as a Graduate Council Fellow. The authors thank Khagendra Baral, Sophia Ezendu, Tristan Maxson, and Ademola Soyemi for their insightful comments on the manuscript. This research used resources of the National Energy Research Scientific Computing Center (NERSC), a U.S. Department of Energy Office of Science User Facility located at Lawrence Berkeley National Laboratory, operated under Contract No. DE-AC02-05CH11231 using NERSC award BES-ERCAP0024218.

Notes and References

- (1) Li, H.; Aguirre-Villegas, H. A.; Allen, R. D.; Bai, X.; Benson, C. H.; Beckham, G. T.; Bradshaw, S. L.; Brown, J. L.; Brown, R. C.; Cecon, V. S. Expanding plastics recycling technologies: chemical aspects, technology status and challenges. *Green Chemistry* **2022**, *24* (23), 8899-9002.
- (2) Lieberzeit, P.; Bekchanov, D.; Mukhamediev, M. Polyvinyl chloride modifications, properties, and applications. *Polymers for Advanced Technologies* **2022**, *33* (6), 1809-1820.
- (3) Lewandowski, K.; Skórczewska, K. A brief review of poly (vinyl chloride)(PVC) recycling. *Polymers* **2022**, *14* (15), 3035.
- (4) Walker, B. North America's Cinderella Pipe Story: A Look at PVC Pipes' Climb to the Top. In *Plastic Pipe and Fittings: Past, Present, and Future*, Walsh, T. Ed.; American Society for Testing and Materials (ASTM International), 2011.
- (5) Świetlik, J.; Magnucka, M. Chemical and microbiological safety of drinking water in distribution networks made of plastic pipes. *Wiley Interdisciplinary Reviews: Water* **2024**, *11* (2), e1704.
- (6) Hu, Q.; Zhang, Z.; He, D.; Wu, J.; Ding, J.; Chen, Q.; Jiao, X.; Xie, Y. Progress and Perspective for "Green" Strategies of Catalytic Plastics

- Conversion into Fuels by Regulating Half-Reactions. *Journal of the American Chemical Society* **2024**, *146* (25), 16950-16962.
- (7) Ezendu, S.; Soyemi, A.; Szilvasi, T. Multiscale Simulation of Plastic Transformations: The Case of Base-Assisted Dehydrochlorination of Polyvinyl Chloride. *ChemRxiv*. **2024**.
- (8) Yoshioka, T.; Kameda, T.; Imai, S.; Okuwaki, A. Dechlorination of poly (vinyl chloride) using NaOH in ethylene glycol under atmospheric pressure. *Polymer degradation and stability* **2008**, *93* (6), 1138-1141.
- (9) Al Alshaikh, A.; Bara, J. E. Chlorinated plastics offer unique opportunities and challenges in upcycling. *Polymer International* **2024**, *73* (5), 341-348. DOI: <https://doi.org/10.1002/pi.6621> (accessed 2024/07/03).
- (10) Bao, J. L.; Truhlar, D. G. Variational transition state theory: theoretical framework and recent developments. *Chemical Society Reviews* **2017**, *46* (24), 7548-7596.
- (11) Greer, E. M.; Siev, V.; Segal, A.; Greer, A.; Doubleday, C. Computational evidence for tunneling and a hidden intermediate in the biosynthesis of tetrahydrocannabinol. *Journal of the American Chemical Society* **2022**, *144* (17), 7646-7656.
- (12) Frenklach, A.; Amlani, H.; Kozuch, S. Quantum Tunneling Instability in Pericyclic Reactions. *Journal of the American Chemical Society* **2024**, *146* (17), 11823 - 11834. DOI: 10.1021/jacs.4c00608.
- (13) Schreiner, P. R. Quantum mechanical tunneling is essential to understanding chemical reactivity. *Trends in Chemistry* **2020**, *2* (11), 980-989.
- (14) Meisner, J.; Kästner, J. Atom tunneling in chemistry. *Angewandte Chemie International Edition* **2016**, *55* (18), 5400-5413.
- (15) Borden, W. T. Reactions that involve tunneling by carbon and the role that calculations have played in their study. *Wiley Interdisciplinary Reviews: Computational Molecular Science* **2016**, *6* (1), 20-46.
- (16) Nandi, A.; Molpeceres, G.; Gupta, P. K.; Major, D. T.; Kästner, J.; Martin, J. M.; Kozuch, S. Quantum Tunneling in Computational Catalysis and Kinetics: Is it Really Important? In *Comprehensive Computational Chemistry*, Elsevier, 2024; pp 713-734.
- (17) Brookes, J. C. Quantum effects in biology: golden rule in enzymes, olfaction, photosynthesis and magnetodetection. *Proceedings of the Royal Society A: Mathematical, Physical and Engineering Sciences* **2017**, *473* (2201), 20160822.
- (18) Allemann, R. K.; Scrutton, N. S. *Quantum tunnelling in enzyme-catalysed reactions*; Royal Society of Chemistry, 2009.
- (19) Castro, C.; Karney, W. L. Heavy-Atom Tunneling in Organic Reactions. *Angewandte Chemie* **2020**, *132* (22), 8431-8442.
- (20) Doubleday, C.; Armas, R.; Walker, D.; Cosgriff, C. V.; Greer, E. M. Heavy-Atom Tunneling Calculations in Thirteen Organic Reactions: Tunneling Contributions are Substantial, and Bell's Formula Closely Approximates Multidimensional Tunneling at ≥ 250 K. *Angewandte Chemie* **2017**, *129* (42), 13279-13282.
- (21) Greer, E. M.; Kwon, K.; Greer, A.; Doubleday, C. Thermally activated tunneling in organic reactions. *Tetrahedron* **2016**, *72* (47), 7357-7373.
- (22) Bennett, C. K.; Bhagat, M. N.; Zhu, Y.; Yu, Y.; Raghuraman, A.; Belowich, M. E.; Nguyen, S. T.; Notestein, J. M.; Broadbelt, L. J. Strong influence of the nucleophile on the rate and selectivity of 1, 2-epoxyoctane ring opening catalyzed by tris (pentafluorophenyl) borane, B (C₆F₅)₃. *ACS Catalysis* **2019**, *9* (12), 11589-11602.
- (23) Guo, W.; Robinson, E. E.; Thomson, R. J.; Tantillo, D. J. Heavy Atom Quantum Mechanical Tunneling in Total Synthesis. *Organic Letters* **2024**, *26* (22), 4606-4609. DOI: 10.1021/acs.orglett.4c01152.
- (24) Jackson, B.; Nave, S. The dissociative chemisorption of methane on Ni (111): The effects of molecular vibration and lattice motion. *The Journal of Chemical Physics* **2013**, *138* (17).
- (25) Kyriakou, G.; Davidson, E. R.; Peng, G.; Roling, L. T.; Singh, S.; Boucher, M. B.; Marcinkowski, M. D.; Mavrikakis, M.; Michaelides, A.; Sykes, E. C. H. Significant quantum effects in hydrogen activation. *ACS nano* **2014**, *8* (5), 4827-4835.
- (26) German, E. D.; Sheintuch, M. Kinetics of Catalytic OH Dissociation on Metal Surfaces. *The Journal of Physical Chemistry C* **2012**, *116* (9), 5700-5709. DOI: 10.1021/jp2106499.
- (27) Cuccato, D.; Dossi, M.; Polino, D.; Cavallotti, C.; Moscatelli, D. Is Quantum Tunneling Relevant in Free-Radical Polymerization? *Macromolecular Reaction Engineering* **2012**, *6* (12), 496-506.
- (28) Purmova, J.; Pauwels, K. F.; Van Zoelen, W.; Vorenkamp, E. J.; Schouten, A. J.; Coote, M. L. New insight into the formation of structural defects in poly (vinyl chloride). *Macromolecules* **2005**, *38* (15), 6352-6366.
- (29) Zhu, Y.; Yang, X.; Yu, F.; Wang, R.; Chen, Q.; Zhang, Z.; Wang, Z. Quantum tunneling of hydrogen atom transfer affects mandrel degradation in inertial confinement fusion target fabrication. *Iscience* **2022**, *25* (1).
- (30) Wentzel, G. Eine verallgemeinerung der quantenbedingungen für die zwecke der wellenmechanik. *Zeitschrift für Physik* **1926**, *38* (6), 518-529.
- (31) Kramers, H. A. Wellenmechanik und halbzahlige Quantisierung. *Zeitschrift für Physik* **1926**, *39* (10), 828-840.
- (32) Brillouin, L. La mécanique ondulatoire de Schrödinger; une méthode générale de résolution par approximations successives. *CR Acad. Sci* **1926**, *183* (11), 24-26.
- (33) Eckart, C. The penetration of a potential barrier by electrons. *Physical Review* **1930**, *35* (11), 1303.
- (34) Truhlar, D. G. Semiclassical Multidimensional Tunnelling Calculations. *Tunnelling in Molecules* **2020**, 261-282.
- (35) Truhlar, D. G.; Garrett, B. C. Variational transition-state theory. *Accounts of Chemical Research* **1980**, *13* (12), 440-448.
- (36) Liu, Y. P.; Lynch, G. C.; Truong, T. N.; Lu, D. H.; Truhlar, D. G.; Garrett, B. C. Molecular modeling of the kinetic isotope effect for the [1, 5]-sigmatropic rearrangement of cis-1, 3-pentadiene. *Journal of the American Chemical Society* **1993**, *115* (6), 2408-2415.
- (37) Chai, J.-D.; Head-Gordon, M. Long-range corrected hybrid density functionals with damped atom-atom dispersion corrections. *Physical Chemistry Chemical Physics* **2008**, *10* (44), 6615-6620, 10.1039/B810189B. DOI: 10.1039/B810189B.
- (38) Clark, T.; Chandrasekhar, J.; Spitznagel, G. W.; Schleyer, P. V. R. Efficient diffuse function-augmented basis sets for anion calculations. III. The 3-21+ G basis set for first-row elements, Li-F. *Journal of Computational Chemistry* **1983**, *4* (3), 294-301.
- (39) McLean, A.; Chandler, G. Contracted Gaussian basis sets for molecular calculations. I. Second row atoms, Z= 11-18. *The Journal of chemical physics* **1980**, *72* (10), 5639-5648.
- (40) Marenich, A. V.; Cramer, C. J.; Truhlar, D. G. Universal solvation model based on solute electron density and on a continuum model of the solvent defined by the bulk dielectric constant and atomic surface tensions. *The Journal of Physical Chemistry B* **2009**, *113* (18), 6378-6396.
- (41) Qiu, G.; Schreiner, P. R. The Intrinsic Barrier Width and Its Role in Chemical Reactivity. *ACS Central Science* **2023**, *9* (11), 2129-2137.
- (42) Kästner, J. Theory and simulation of atom tunneling in chemical reactions. *Wiley Interdisciplinary Reviews: Computational Molecular Science* **2014**, *4* (2), 158-168.

The data supporting this article have been included as part of the Supplementary Information.